

Spectral properties of quantum N -body systems *versus* chaotic properties of their mean field approximations

Patrizia Castiglione,^a Giovanni Jona-Lasinio,^b and Carlo Presilla^c
Dipartimento di Fisica, Università di Roma "La Sapienza,"
Piazzale A. Moro 2, 00185 Roma, Italy
(cond-mat/9604084 submitted to J. Phys. A)

We present numerical evidence that in a system of interacting bosons there exists a correspondence between the spectral properties of the exact quantum Hamiltonian and the dynamical chaos of the associated mean field evolution. This correspondence, analogous to the usual quantum-classical correspondence, is related to the formal parallel between the second quantization of the mean field, which generates the exact dynamics of the quantum N -body system, and the first quantization of classical canonical coordinates. The limit of infinite density and the thermodynamic limit are then briefly discussed.

05.45.+b, 03.65.-w, 73.40.Gk

I. INTRODUCTION

The commonly accepted definition of *quantum chaos* is based on universal statistical properties of suitably defined fluctuations in the energy spectrum. For instance, a confined quantum system with a finite number of degrees of freedom, e.g., a particle in a billiard, is said to be chaotic whenever the nearest neighbor level spacing (NNLS) distribution, with the spacings normalized to their local average value, is well approximated by the corresponding Wigner distribution for random matrices [1].

This definition of quantum chaos was conjectured [2] to satisfy a correspondence principle with the *dynamical chaos* of the associated classical system, i.e., the exponential sensitivity of the classical trajectories to a variation of the initial conditions. In fact, a large collection of numerical examples [3] shows that, whenever the classical system has positive (non positive) maximum Lyapunov exponent, the corresponding quantum system has Wigner-like (non Wigner-like) NNLS distribution. The recent result [4] gives a theoretical support to this conjecture.

In the case of systems made of N identical particles nonlinearly interacting, quantum chaos, in the sense stated above, seems a general rule [5–7]. For these systems, we suggest to look for a correspondence of the quantum chaos with the dynamical chaos of associated c -number canonical coordinates well distinguished from the classical ones. These c -number canonical coordinates are appropriate combinations of time-dependent mean fields which approximate the dynamics of the N -body symmetrized or antisymmetrized wavefunction [8]. The dynamical equations of the mean fields are, in general, nonlinear and allow the presence of dynamical chaos as in classical mechanics [9]. A *second quantization* transforms the mean fields into field operators and restores the exact dynamics of the quantum N -body system. This second quantization can be made formally identical to the quantization of classical canonical coordinates and, by analogy, we can expect a correspondence between quantum chaos of N -body systems and dynamical chaos of their mean field approximations.

In this paper, we numerically investigate a system of N bosons with both periodic and Dirichlet boundary conditions. In Section II, we analyze the exact system from the point of view of quantum chaos and find that a Wigner-like NNLS distribution is a general feature in presence of nonlinear interaction already for very low values of N . In Section III, we study time-dependent mean field approximations of the same system from the point of view of the exponential sensitivity to the initial conditions. We find that the mean fields show dynamical chaos in correspondence to the quantum chaos of the exact system for all the values of N considered. We naturally assume that this correspondence continues to hold as N increases. In Section IV we quantize the mean field and in the last Section we discuss the limit of infinite density and the thermodynamic limit.

II. THE MODEL AND ITS PROPERTIES

Let us consider a system of N spinless bosons of charge q moving in a one-dimensional lattice with L sites and described by the Hamiltonian

$$\hat{H} = \sum_{j=1}^L \left[\alpha_j \hat{a}_j^\dagger \hat{a}_j - \beta_j \left(e^{i\theta} \hat{a}_{j+1}^\dagger \hat{a}_j + e^{-i\theta} \hat{a}_j^\dagger \hat{a}_{j+1} \right) \right] + \sum_{j=1}^L \gamma_j \hat{a}_j^\dagger \hat{a}_j^\dagger \hat{a}_j \hat{a}_j, \quad (1)$$

where index correspondence $j \pm L = j$ is assumed. The operator \hat{a}_j^\dagger creates a boson in the site j and α_j , β_j , and γ_j are the site, hopping, and interaction energies, respectively. Periodic and Dirichlet boundary conditions will be considered. In the first case, the system represents a ring threaded by a line of magnetic flux ϕ and the phase factors are $\theta = 2\pi\phi/\phi_0 L$, where $\phi_0 = hc/q$ is the flux quantum (in Gauss electromagnetic system). In the second case, the sites lie on a segment and we put $\beta_L = 0$ and $\theta = 0$. The system (1) has wide interest. Its time-dependent mean-field approximation has applications to molecular dynamics and nonlinear optics [10] and to electron transport in heterostructures [11].

All properties of the system (1) can be evaluated by knowing eigenvalues and eigenvectors of \hat{H} . It is simple to work in the space spanned by the Fock states $|n_1^i \cdots n_L^i\rangle$, where n_j^i is the number of bosons in the site j and $\sum_{j=1}^L n_j^i = N$. The index i runs from 1 to the Fock dimension

$$D = \frac{(N + L - 1)!}{N! (L - 1)!} \quad (2)$$

obtained by counting all the possible arrangements of the N identical bosons into the L sites. The D -dimensional matrix H representing the Hamiltonian (1) in the Fock basis has matrix elements

$$H_{ki} = \langle n_1^k \cdots n_L^k | \hat{H} | n_1^i \cdots n_L^i \rangle = \sum_{j=1}^L [\alpha_j n_j^i + \gamma_j n_j^i (n_j^i - 1)] \delta_{ki} + \sum_{j=1}^L \beta_j \left[e^{i\theta} \sqrt{n_j^i (n_{j+1}^i + 1)} \Delta_{ki}(j) + e^{-i\theta} \sqrt{n_{j+1}^i (n_j^i + 1)} \Delta_{ik}(j) \right], \quad (3)$$

where

$$\Delta_{ki}(j) = \begin{cases} 1 & \text{if } n_j^k = n_j^i + 1, n_{j+1}^k = n_{j+1}^i - 1, \text{ and } n_l^k = n_l^i \text{ for } l \neq j, j+1, \\ 0 & \text{otherwise.} \end{cases} \quad (4)$$

The eigenvalues E_i and eigenvectors $|E_i\rangle$ of the Hermitian matrix (3) can be numerically evaluated with standard methods [12]. A bound to the maximum dimension D that can be studied is essentially fixed only by the computer memory necessary to storage the full sparse matrix (3).

For a general, asymmetric system, the NNLS distribution is evaluated from all the eigenvalues E_i . The normalized spacings between nearest neighbor levels, whose distribution $P(s)$ is of interest, are taken as

$$s_i = (E_{i+1} - E_i) / \Delta E_{\text{av}}(i), \quad (5)$$

where

$$\Delta E_{\text{av}}(i) = \frac{1}{2N_{\text{av}} + 1} \sum_{k=-N_{\text{av}}}^{N_{\text{av}}} (E_{i+k+1} - E_{i+k}) \quad (6)$$

with $1 \ll N_{\text{av}} \ll D$. In the case of Dirichlet boundary conditions, the Hamiltonian matrix is real symmetric and correspondence to the Gaussian orthogonal ensemble (GOE) of random matrices may be expected. In the case of periodic boundary conditions, the Hamiltonian matrix is complex Hermitian and, in general, correspondence to the Gaussian unitary ensemble (GUE) may be expected. However, if the external potential, represented by the site energies α_j , is symmetric under a reflection with respect to some diameter of the ring, the system has an anti-unitary symmetry and GOE behavior is restored [13].

In presence of geometrical symmetries, the level statistics analysis probing the phenomenon of level repulsion is meaningful only once the trivial crossings of eigenvalues belonging to different symmetry classes are avoided [14]. This amounts to analyze the NNLS distribution separately inside each one of the diagonal blocks which compose the matrix H in a proper basis. For example, a uniform system, i.e., a system with α_j , β_j , and γ_j independent of the site-index j , is invariant under rotation

$$\hat{\mathcal{R}} : j \mapsto j + 1 \quad (7)$$

in the case of periodic boundary conditions, and space-inversion

$$\hat{\mathcal{P}} : j \mapsto L + 1 - j \quad (8)$$

in the case of Dirichlet boundary conditions. The eigenvalues of \hat{H} must be divided into L classes, corresponding to the eigenvalues $\exp(i2\pi\nu/L)$, with $\nu = 1, \dots, L$, of $\hat{\mathcal{R}}$, in the first case, and into two classes, corresponding to the eigenvalues ± 1 of $\hat{\mathcal{P}}$, in the second one. This is accomplished by evaluating the operator \hat{H} in the basis of the degenerate eigenvectors of $\hat{\mathcal{R}}$ or $\hat{\mathcal{P}}$ in which the corresponding matrix H is block-diagonal. Each block is then independently diagonalised to find the eigenvalues of H within the corresponding symmetry class.

The eigenvectors $|\nu_q\rangle$ of $\hat{\mathcal{R}}$, q being the degeneracy index, are obtained by numerically solving the eigenvalue problem

$$\sum_{i=1}^D (\mathcal{R}_{ki} - \lambda_\nu \delta_{ki}) \langle n_1^i \cdots n_L^i | \nu_q \rangle = 0 \quad (9)$$

where

$$\mathcal{R}_{ki} = \langle n_1^k \cdots n_L^k | \hat{\mathcal{R}} | n_1^i \cdots n_L^i \rangle = \begin{cases} 1 & \text{if } n_j^k = n_{j+1}^i \text{ for } j = 1, \dots, L, \\ 0 & \text{otherwise.} \end{cases} \quad (10)$$

The block of H corresponding to the eigenvalue $\lambda_\nu = \exp(i2\pi\nu/L)$ has matrix elements

$$H_{\nu_q \nu_p} = \sum_{k,i=1}^D \langle \nu_q | n_1^k \cdots n_L^k \rangle H_{ki} \langle n_1^i \cdots n_L^i | \nu_p \rangle. \quad (11)$$

A similar, general procedure could be applied also to $\hat{\mathcal{P}}$. However, the eigenvectors of $\hat{\mathcal{P}}$ are, by inspection, single Fock states or symmetric and antisymmetric combinations of couples of Fock states. The even and odd blocks of H , corresponding to the eigenvalues ± 1 of $\hat{\mathcal{P}}$, have matrix elements which are straightforward combinations of those in (3).

Figure 1 shows the NNLS distribution obtained for a uniform system with periodic and Dirichlet boundary conditions. The distributions of the normalized spacings (5) evaluated for each symmetry class of eigenvalues have been summed up for increasing the statistical confidence. The agreement of the calculated NNLS distribution with the Wigner surmise for the GOE distribution $P_{\text{GOE}}(s) = (\pi s/2) \exp(-\pi s^2/4)$, also shown in the same figure, is statistically reliable.

The importance of performing the level statistics analysis within the appropriate symmetry classes is evidenced in Fig. 2, where the NNLS distribution for the same uniform systems of Fig. 1 is evaluated from the total spectrum of \hat{H} . In the case of Dirichlet boundary conditions, the mixing of the even- and odd-parity eigenvalues generates a two-peaks distribution which behaves like $\exp(-s)$ at large s . In the case of periodic boundary conditions, due to the higher number of symmetry classes and their statistical independence, we observe a distribution which mimics the Poisson distribution $P_{\text{P}}(s) = \exp(-s)$ even at small s [14]. This fact and the observation that similar results are obtained when the symmetries are only approximate [5], will be relevant in the following.

The above mentioned geometrical symmetries can be explicitly broken by choosing an appropriate j -dependence in the parameters α_j , β_j , and γ_j . Figure 3 shows the NNLS distribution obtained with periodic boundary conditions when the site energies have the form $\alpha_j = 2(N-1)\eta \xi_j$, where ξ_j are arbitrary positive numbers with $\sum_{j=1}^L \xi_j = 1$, and all the other parameters are as in the uniform case. The resemblance of the calculated distribution with the GUE Wigner surmise, $P_{\text{GUE}}(s) = (32s^2/\pi^2) \exp(-4s^2/\pi)$, expected on the base of the complex Hermitian nature of H , is statistically reliable. However, the GOE behavior is restored, as shown in Fig. 4, by choosing ξ_j symmetric with respect to an arbitrary j_0 . Figures 5 and 6 show the NNLS distribution obtained when the hopping and interaction energies have the form indicated in the captions and the other parameters are as in the uniform case. The calculated distribution is always close to the GOE one for both periodic and Dirichlet boundary conditions.

Results similar to those discussed above are obtained for other choices of the parameters, N , L , α_j , β_j , γ_j , and ϕ i.e., the system (1) is generally characterized by a Wigner-like NNLS distribution. Integrability points are the only exception to this rule. A first, trivial, point of integrability of the system (1) is the noninteracting case obtained for $\gamma_j \rightarrow 0$ with eigenvalues given by $E_i = \sum_{j=1}^L \epsilon_j n_j^i$, ϵ_j being the L eigenvalues obtained for $N = 1$. A second point is approached for $\beta_j \rightarrow 0$ with eigenvalues given by $E_i = \sum_{j=1}^L \alpha_j n_j^i + \gamma_j n_j^i (n_j^i - 1)$. A third point of integrability is obtained by taking the continuum limit in which Eq. (1) becomes the second quantization version of the Hamiltonian of N bosons interacting via a δ -function potential

$$\sum_{n=1}^N \left[-\frac{\hbar^2}{2m} \frac{\partial^2}{\partial x_n^2} + C \sum_{n'=n+1}^N \delta(x_n - x_{n'}) \right] \quad (12)$$

with $0 \leq x_n \leq \ell$. This system is solvable by the Bethe ansatz [15] and can be obtained from (1) by putting $\alpha_j = 2\beta_j = \hbar^2/(m\Delta x^2)$ and $\gamma_j = C/\Delta x$ with $\Delta x = \ell/L$ and letting $L \rightarrow \infty$. When approaching an integrability point, the NNLS distribution transforms into a non Wigner-like distribution whose shape strongly depends on the values of the system parameters.

The results of the level statistics analysis obtained for the boson system (1) are in agreement with those found in [5–7] for fermion systems. Quantum chaos, in the sense stated in the Introduction, is a generic feature of systems with many particles nonlinearly interacting. The only apparent exception to this rule is a result of [7] in which a system of spinless electrons moving in a ring similar to ours is shown to have Poisson-like NNLS distribution whenever the interaction is limited to a small region of the ring. However, studying the same fermion system we found that the case considered in [7] has an approximate symmetry [16]. When this symmetry is taken into account or is removed by changing the relevant parameters, e.g., adding a random energy to the sites, the NNLS distribution turns to a GOE distribution as in the example of Fig. 6.

III. MEAN FIELD APPROXIMATION

Two substantially equivalent time-dependent mean field approximations of the Hamiltonian (1) are obtained by choosing the N particles to be described by the normalized boson condensate

$$|Z_N(t)\rangle = (N!)^{-1/2} [\hat{a}_z^\dagger(t)]^N |\mathbf{0}\rangle \quad (13)$$

or the normalized coherent state

$$|Z_N(t)\rangle = \exp \left[\sqrt{N} \hat{a}_z^\dagger(t) - \sqrt{N} \hat{a}_z(t) \right] |\mathbf{0}\rangle. \quad (14)$$

Here, $|\mathbf{0}\rangle$ is the vacuum state and $\hat{a}_z^\dagger(t)$ creates a boson in the single-particle state

$$|z(t)\rangle = \hat{a}_z^\dagger(t) |\mathbf{0}\rangle = \sum_{j=1}^L z_j(t) \hat{a}_j^\dagger |\mathbf{0}\rangle = \sum_{j=1}^L z_j(t) |j\rangle. \quad (15)$$

The normalization condition of this state, $\langle z(t)|z(t)\rangle = \sum_{j=1}^L |z_j(t)|^2 = 1$, fixes the expectation number of particles in the boson condensate (13) or the coherent state (14) to N since in both cases we have $\langle Z_N(t) | \hat{a}_j^\dagger \hat{a}_j | Z_N(t) \rangle = N |z_j(t)|^2$. The time evolution of the complex amplitudes $z_j(t) = \langle j | z(t) \rangle$ is obtained from a variational principle for the Dirac action [8]

$$\int dt \langle Z_N(t) | i\hbar \frac{d}{dt} - \hat{H} | Z_N(t) \rangle. \quad (16)$$

For a general Hamiltonian $\hat{H} = \hat{T} + \hat{V}$, sum of a single-particle term \hat{T} and a two-particle term \hat{V} ,

$$\hat{H} = \sum_{kn} T_{kn} \hat{a}_k^\dagger \hat{a}_n + \frac{1}{2} \sum_{kk'nn'} V_{kk'nn'} \hat{a}_k^\dagger \hat{a}_{k'}^\dagger \hat{a}_n \hat{a}_{n'}, \quad (17)$$

we have

$$\begin{aligned} \langle Z_N(t) | i\hbar \frac{d}{dt} - \hat{H} | Z_N(t) \rangle &= i\hbar \sum_k N \bar{z}_k(t) \frac{d}{dt} z_k(t) - \sum_{kn} T_{kn} N \bar{z}_k(t) z_n(t) \\ &\quad - \frac{1}{2} \sum_{kk'nn'} V_{kk'nn'} N(N-1) \bar{z}_k(t) \bar{z}_{k'}(t) z_n(t) z_{n'}(t). \end{aligned} \quad (18)$$

In the above expression as well as in the following ones of this Section, we use the boson condensate (13). Similar expressions hold for the coherent state (14) with the substitution $(N-1) \rightarrow N$. The action (16) is stationary with respect to a variation of $\bar{z}_j(t)$ if

$$i\hbar \frac{d}{dt} z_j(t) = \sum_l h_{jl}[z(t)] z_l(t) \quad (19)$$

where

$$h_{jl}[z(t)] = T_{jl} + (N-1) \sum_{kn} V_{jkl n} \bar{z}_k(t) z_n(t) \quad (20)$$

are the matrix elements of the mean field single-particle Hamiltonian $h[z(t)]$. In the case of the Hamiltonian (1), we have

$$T_{jl} = \alpha_j \delta_{jl} - \beta_l e^{i\theta} \delta_{j,l+1} - \beta_j e^{-i\theta} \delta_{j+1,l}, \quad (21)$$

$$V_{jkl n} = 2\gamma_j \delta_{jk} \delta_{kl} \delta_{ln} \quad (22)$$

and the mean field single-particle Hamiltonian has matrix elements

$$h_{jl}[z(t)] = \alpha_j \delta_{jl} - \beta_l e^{i\theta} \delta_{j,l+1} - \beta_j e^{-i\theta} \delta_{j+1,l} + 2(N-1)\gamma_j |z_j(t)|^2 \delta_{jl} \quad (23)$$

with $j, l = 1, \dots, L$.

The system of nonlinear Schrödinger equations (19) with $h_{jl}[z(t)]$ given by (23) must be numerically solved starting from initial values $z_j(0)$ with the normalization condition $\sum_{j=1}^L |z_j(0)|^2 = 1$. The choice of the numerical algorithm is critically related to the existence of conservation laws. By inspection, the system (19) has two conserved quantities, the single-particle probability

$$\|z(t)\|^2 \equiv \sum_{j=1}^L |z_j(t)|^2 \quad (24)$$

and the single-particle energy

$$\mathcal{E}[z, \bar{z}] = \sum_{j=1}^L \left\{ \alpha_j |z_j(t)|^2 - [\beta_{j-1} e^{i\theta} z_{j-1}(t) + \beta_j e^{-i\theta} z_{j+1}(t)] \bar{z}_j(t) + (N-1)\gamma_j |z_j(t)|^4 \right\}. \quad (25)$$

The conservation law (24) suggests the use a finite-difference Crank-Nicholson scheme [12]

$$\sum_{l=1}^L \left(\delta_{jl} + i \frac{\Delta t}{2\hbar} h_{jl}[z(t+\Delta t)] \right) z_l(t+\Delta t) = \sum_{l=1}^L \left(\delta_{jl} - i \frac{\Delta t}{2\hbar} h_{jl}[z(t)] \right) z_l(t) \quad (26)$$

which is simple to handle numerically due to the tridiagonal nature of the matrix h [17]. The above scheme would be correct $\mathcal{O}(\Delta t^2)$ if the matrix h were time independent. However, this is not our case and we have to approximate the matrix elements in the l.h.s. of (26). The simple approximation $h_{jl}[z(t+\Delta t)] \simeq h_{jl}[z(t)]$ has catastrophic effects for the conservation law (25) unless very small values of Δt are chosen. An improvement is obtained with an iterative procedure. Let us suppose $z_j(t)$ known and try

$$z_j(t+\Delta t) = \lim_{n \rightarrow \infty} z_j^{(n)}(t+\Delta t). \quad (27)$$

The $n=0$ term is defined by solving

$$\sum_{l=1}^L \left(\delta_{jl} + i \frac{\Delta t}{2\hbar} h_{jl}[z(t)] \right) z_l^{(0)}(t+\Delta t) = \sum_{l=1}^L \left(\delta_{jl} - i \frac{\Delta t}{2\hbar} h_{jl}[z(t)] \right) z_l(t) \quad (28)$$

and the $n \geq 1$ terms are chosen as solutions of

$$\sum_{l=1}^L \left(\delta_{jl} + i \frac{\Delta t}{2\hbar} h_{jl}[z^{(n-1)}(t+\Delta t)] \right) z_l^{(n)}(t+\Delta t) = \sum_{l=1}^L \left(\delta_{jl} - i \frac{\Delta t}{2\hbar} h_{jl}[z(t)] \right) z_l(t). \quad (29)$$

This iterative scheme converges in very few steps and ensures an excellent conservation of both quantities (24) and (25).

The system (19) can show local exponential instability. The corresponding maximum Lyapunov exponent λ defined by

$$\lambda = \lim_{t \rightarrow \infty} \Lambda(t), \quad \Lambda(t) \equiv \frac{1}{t} \ln \frac{\|\delta z(t)\|}{\|\delta z(0)\|}, \quad (30)$$

measures the exponential separation between two states $|z(t)\rangle$ and $|z(t)\rangle + \epsilon|\delta z(t)\rangle$ infinitesimally close ($\epsilon \rightarrow 0$). The site projections $\delta z_j(t) = \langle j|\delta z(t)\rangle$ satisfy the set of equations obtained by linearizing (19)

$$i\hbar \frac{d}{dt} \delta z_j(t) = \sum_{l=1}^L h_{jl}[z(t)] \delta z_l(t) + P[z_j(t), \delta z_j(t), \delta \bar{z}_j(t)], \quad (31)$$

where

$$P[z_j(t), \delta z_j(t), \delta \bar{z}_j(t)] = 2(N-1)\gamma_j z_j(t) [z_j(t)\delta \bar{z}_j(t) + \bar{z}_j(t)\delta z_j(t)], \quad (32)$$

and can be evaluated by numerically integrating (31) simultaneously with (19). The initial values $\delta z_j(0)$ can not be chosen arbitrarily. Indeed, the state $|z(t)\rangle + \epsilon|\delta z(t)\rangle$ must be normalized up to terms $\mathcal{O}(\epsilon^2)$. Since $\|z(t)\| = 1$, we must have $\text{Re}\langle z(t)|\delta z(t)\rangle = 0$ at any time. However, by using (19) and (31) we have

$$\frac{d}{dt} \text{Re}\langle z(t)|\delta z(t)\rangle = \text{Re} \sum_{j=1}^L \left[\delta z_j(t) \frac{d}{dt} \bar{z}_j(t) + \bar{z}_j(t) \frac{d}{dt} \delta z_j(t) \right] = 0 \quad (33)$$

and, therefore, it is sufficient to have $\text{Re}\langle z(0)|\delta z(0)\rangle = 0$.

For solving (31) simultaneously with (19) we again adopt an iterative modification of the Crank-Nicholson scheme in which P is considered as a driving term. Let us suppose $z_j(t)$ and $\delta z_j(t)$ known and try

$$\delta z_j(t + \Delta t) = \lim_{n \rightarrow \infty} \delta z_j^{(n)}(t + \Delta t). \quad (34)$$

The $n = 0$ term is defined by solving

$$\begin{aligned} \sum_{l=1}^L \left(\delta_{jl} + i \frac{\Delta t}{2\hbar} h_{jl}[z(t)] \right) \delta z_l^{(0)}(t + \Delta t) &= \sum_{l=1}^L \left(\delta_{jl} - i \frac{\Delta t}{2\hbar} h_{jl}[z(t)] \right) \delta z_l(t) \\ &- i \frac{\Delta t}{2\hbar} \left(P[z_j(t), \delta z_j(t), \delta \bar{z}_j(t)] + P[z_j(t), \delta z_j(t), \delta \bar{z}_j(t)] \right) \end{aligned} \quad (35)$$

and the $n \geq 1$ terms are chosen as solution of

$$\begin{aligned} \sum_{l=1}^L \left(\delta_{jl} + i \frac{\Delta t}{2\hbar} h_{jl}[z^{(n-1)}(t)] \right) \delta z_l^{(n)}(t + \Delta t) &= \sum_{l=1}^L \left(\delta_{jl} - i \frac{\Delta t}{2\hbar} h_{jl}[z(t)] \right) \delta z_l(t) \\ &- i \frac{\Delta t}{2\hbar} \left(P[z_j^{(n-1)}(t + \Delta t), \delta z_j^{(n-1)}(t + \Delta t), \delta \bar{z}_j^{(n-1)}(t + \Delta t)] + P[z_j(t), \delta z_j(t), \delta \bar{z}_j(t)] \right). \end{aligned} \quad (36)$$

Note that (36) must be solved after (29) and (36) have been solved at the iteration $n - 1$ in order to know both $z_j^{(n-1)}(t + \Delta t)$ and $\delta z_j^{(n-1)}(t + \Delta t)$.

The quantity $\|\delta z(t)\|$ can grow exponentially and, therefore, $\delta z_j(t)$ must be periodically scaled in order to avoid numerical overflows [18]. The scaling factors are stored for computing the Lyapunov exponent (30). When the system (19) is chaotic, the computer round-off errors inevitably make the numerical solutions obtained with different integration steps Δt different after a sufficiently long time. Therefore, the comparison of solutions relative to different steps is not a good check that the algorithm correctly works, unless time-averaged quantities, e.g., the Lyapunov exponent (30), are compared [19]. On the other hand, a check based on the conservation of the quantities (24) and (25) is meaningful and can be used to fix the size of the integration step in relation to a chosen accuracy. With the modified Crank-Nicholson scheme described above, for $\Delta t \lesssim 10^{-3}\hbar/\eta$ after 10^8 iterations we have relative errors in (24) and (25) which are smaller than 10^{-5} and 10^{-4} , respectively.

Figures 7 and 8 show the behavior of $\Lambda(t)$ with periodic and Dirichlet boundary conditions, respectively. The curves denoted with u , α , β , and γ , refer to the system in which all the parameters are independent of j as in Fig. 1, α_j is random as in Fig. 3, β_j is as in Fig. 5, and γ_j is localized as in Fig. 6, respectively. After an initial transient, not shown in Figs. 7 and 8, $\Lambda(t)$ approximately stabilizes around a positive value which we take as the corresponding maximum Lyapunov exponent λ . Note that $\lambda^{-1} \lesssim 10^2 \hbar / \eta$ is much smaller than the maximum simulation time $10^5 \hbar / \eta$. The value of λ is independent of changes in the initial conditions $\delta z_j(0)$. It is also independent of changes in the initial conditions $z_j(0)$ provided that the conserved energy $\mathcal{E}[z, \bar{z}]$ is not changed. The maximum Lyapunov exponent exceptionally vanishes when the initial state $|z(0)\rangle$ is coincident or very close to one of the stationary states of the system (19) which are defined by

$$|z_E(t)\rangle = e^{-\frac{i}{\hbar}Et}|z_E(0)\rangle, \quad \|z_E(t)\|^2 = 1. \quad (37)$$

The comparison of Figs. 1-6 with Figs. 7-8 suggests a correspondence between quantum chaos of a system of interacting particles and dynamical chaos of its mean field approximations. Whenever the exact system (1) shows Wigner-like NNLS distribution the corresponding mean field system (19), or that for the coherent state (14), has a positive maximum Lyapunov exponent.

The simultaneous presence of chaotic behavior in the exact and mean-field systems is obtained also for values of the parameters N , L , α_j , β_j , γ_j , and ϕ different from those reported. In the three cases in which the exact system has been shown to be integrable, namely $\gamma_j \rightarrow 0$, $\beta_j \rightarrow 0$, and the continuum limit, the corresponding mean field system is integrable and has $\lambda = 0$. For $\gamma_j \rightarrow 0$, the system (19) becomes linear and $\Lambda(t) \equiv 0$. For $\beta_j \rightarrow 0$, we have

$$\frac{d}{dt}|z_j(t)|^2 = z_j(t)\frac{d}{dt}\bar{z}_j(t) + \bar{z}_j(t)\frac{d}{dt}z_j(t) = 0 \quad (38)$$

and, therefore,

$$z_j(t) = z_j(0)e^{-i(\alpha_j + 2(N-1)\gamma_j|z_j(0)|^2)t/\hbar}. \quad (39)$$

The corresponding variation

$$\begin{aligned} \delta z_j(t) &= \delta z_j(0)e^{-i(\alpha_j + 2(N-1)\gamma_j|z_j(0)|^2)t/\hbar} \\ &\quad - z_j(0)i\frac{t}{\hbar}2(N-1)\gamma_j[\delta z_j(0)\bar{z}_j(0) + z_j(0)\delta\bar{z}_j(0)]e^{-i(\alpha_j + 2(N-1)\gamma_j|z_j(0)|^2)t/\hbar} \end{aligned} \quad (40)$$

shows that $\|\delta z(t)\|$ is $\mathcal{O}(t)$ and therefore $\lambda = 0$. Finally, in the continuum limit the system (19) becomes the well known nonlinear Schrödinger equation,

$$i\hbar\frac{\partial}{\partial t}z(x,t) = -\frac{\hbar^2}{2m}\frac{\partial^2}{\partial x^2}z(x,t) + C(N-1)|z(x,t)|^2z(x,t), \quad (41)$$

solvable via spectral transform [20].

IV. SECOND QUANTIZATION OF THE MEAN FIELD

The correspondence between quantum chaos of an exact N -body system and dynamical chaos of the associated mean field approximations parallels the correspondence between quantum chaos of a single-particle system and dynamical chaos of the associated classical equations. This parallel can be connected to the fact that the first quantization of the classical canonical coordinates has a formal counterpart in the second quantization of the mean field [8]. Let us see this in detail. The mean field $Z_j(t) = \sqrt{N}z_j(t)$, $j = 1, \dots, L$, is determined by the dynamical equation

$$i\hbar\frac{d}{dt}Z_j(t) = \alpha_j Z_j(t) - \beta_{j-1}e^{i\theta}Z_{j-1}(t) - \beta_j e^{-i\theta}Z_{j+1}(t) + 2\gamma_j\bar{Z}_j(t)Z_j(t)Z_j(t). \quad (42)$$

In this Section we will consider the coherent state (14) but similar results hold for the boson condensate (13) with the substitution $N \rightarrow (N-1)$. The quantization rule

$$Z_j(t) \rightarrow \hat{Z}_j(t), \quad \bar{Z}_j(t) \rightarrow \hat{Z}_j^\dagger(t), \quad (43)$$

with

$$\left[\hat{Z}_j(t), \hat{Z}_k(t) \right] = \left[\hat{Z}_j^\dagger(t), \hat{Z}_k^\dagger(t) \right] = 0, \quad \left[\hat{Z}_j(t), \hat{Z}_k^\dagger(t) \right] = \delta_{jk} \quad (44)$$

transforms the nonlinear Schrödinger equation (42) into the Heisenberg equation for the field operator $\hat{Z}_j(t)$. Indeed, in the representation of the site-localized states $\phi_j^k = \delta_{jk}$, we have $\hat{Z}_j(t) = \sum_{k=1}^L \phi_j^k \hat{a}_k(t) = \hat{a}_j(t)$ whose Heisenberg equation of motion is

$$\begin{aligned} i\hbar \frac{d}{dt} \hat{a}_j(t) &= \left[\hat{a}_j(t), \hat{H}(t) \right] \\ &= \alpha_j \hat{a}_j(t) - \beta_{j-1} e^{i\theta} \hat{a}_{j-1}(t) - \beta_j e^{-i\theta} \hat{a}_{j+1}(t) + 2\gamma_j \hat{a}_j^\dagger(t) \hat{a}_j(t) \hat{a}_j(t). \end{aligned} \quad (45)$$

The second quantization (44) can be made formally identical to the first quantization of classical canonical coordinates with the standard transformation

$$Q_j(t) = \sqrt{\frac{\hbar}{2}} \left(Z_j(t) + \bar{Z}_j(t) \right), \quad P_j(t) = \frac{1}{i} \sqrt{\frac{\hbar}{2}} \left(Z_j(t) - \bar{Z}_j(t) \right). \quad (46)$$

By using the total energy of the system

$$\begin{aligned} \mathcal{H}[Q, P] &= N\mathcal{E}[z(Q, P), \bar{z}(Q, P)] \\ &= \sum_{j=1}^L \left\{ \alpha_j \frac{Q_j(t)^2 + P_j(t)^2}{2\hbar} - \left[\beta_{j-1} e^{i\theta} \frac{Q_{j-1}(t) + iP_{j-1}(t)}{\sqrt{2\hbar}} \right. \right. \\ &\quad \left. \left. + \beta_j e^{-i\theta} \frac{Q_{j+1}(t) + iP_{j+1}(t)}{\sqrt{2\hbar}} \right] \frac{Q_j(t) - iP_j(t)}{\sqrt{2\hbar}} + \gamma_j \left(\frac{Q_j(t)^2 + P_j(t)^2}{2\hbar} \right)^2 \right\}, \end{aligned} \quad (47)$$

the nonlinear Schrödinger equation (42) can be rewritten in the Hamilton formalism

$$\frac{d}{dt} Q_j(t) = \frac{d}{dP_j(t)} \mathcal{H}[Q, P], \quad \frac{d}{dt} P_j(t) = -\frac{d}{dQ_j(t)} \mathcal{H}[Q, P] \quad (48)$$

and the quantization (44) is equivalent to the introduction of Hermitian operators $\hat{Q}_j(t)$ and $\hat{P}_j(t)$ with commutation relations

$$\left[\hat{Q}_j(t), \hat{Q}_k(t) \right] = \left[\hat{P}_j(t), \hat{P}_k(t) \right] = 0, \quad \left[\hat{Q}_j(t), \hat{P}_k(t) \right] = i\hbar \delta_{jk}. \quad (49)$$

V. THE LIMIT $N \rightarrow \infty$

We first analyze the limit of infinite density, in which $N \rightarrow \infty$ with L constant.

In this limit the quantum theory reduces to a c -number theory and is, therefore, analogous to a classical limit even though $\hbar \neq 0$ [22]. For our system this is easily seen by retracing the N dependence in the equations of the previous section. For large N , the system reduces to a collection of independent nonlinear oscillators whose nonlinearity grows like N . From the point of view of chaotic properties, the limit $N/L \rightarrow \infty$ is therefore trivial. An example where the same kind of limit gives rise to a non trivial chaotic system can be found in [21].

It is interesting to see the emergence of the limiting behavior $N/L \rightarrow \infty$ by comparing the cumulative density of states

$$D(E) = \text{Tr} \theta(E - \hat{H}) = \sum_{i=1}^D \theta(E - E_i) \quad (50)$$

with the approximate expression obtained according to the Weyl rule

$$D_{\text{mf}}(E) = \frac{1}{(2\pi\hbar)^L} \int dQ_1 \cdots dQ_L \int dP_1 \cdots dP_L \theta(E - \mathcal{H}[Q, P]) \delta(N - \mathcal{N}[Q, P]). \quad (51)$$

Note that we have a δ -function constraint on the $Q - P$ phase space which fixes

$$\mathcal{N}[Q, P] \equiv \sum_{j=1}^L \frac{Q_j(t)^2 + P_j(t)^2}{2\hbar} = N \quad (52)$$

in agreement with (24). Due to the presence of this constraint, the r.h.s. of (51) is a $(2L - 1)$ -multiple integral which can be evaluated with Monte Carlo integration in the hypercube of side $2\sqrt{2\hbar N}$ centered in the origin. Figures 9-11 show, in a case with Dirichlet boundary conditions, that when the density $\rho = N/L$ is increased $D(E)$ is approximated by $D_{\text{mf}}(E)$ with increasing precision. Similar behavior is obtained with periodic boundary conditions and/or different values of the parameters of the system. The total number of levels given by (50) and (51) become equal in the limit $N/L \rightarrow \infty$. Indeed, we have

$$D_{\text{mf}} \equiv \lim_{E \rightarrow \infty} D_{\text{mf}}(E) = \frac{N^{L-1}}{\pi^L} \int dx_1 \dots dx_{2L} \delta \left(1 - \sum_{j=1}^{2L} x_j^2 \right) = \frac{N^{L-1}}{(L-1)!} \quad (53)$$

which is the value of the Fock dimension (2) for $N \gg L$.

For a single-particle system, the smooth behavior of the cumulative density of states is approximated by the corresponding semiclassical expression in the limit of high energies ($\hbar \rightarrow 0$). Analogously, in the case of an N -body system for N/L large we can use $D_{\text{mf}}(E)$ to approximate the smooth behavior of $D(E)$ and evaluate the normalized spacings (5) according to

$$s_i = (E_{i+1} - E_i) \frac{d}{dE} D_{\text{mf}}(E) \simeq D_{\text{mf}}(E_{i+1}) - D_{\text{mf}}(E_i), \quad (54)$$

as suggested in [5].

Finally, let us briefly discuss the thermodynamic limit. Unlike the limit $N/L \rightarrow \infty$, the system preserves its quantum features and the mean fields do not give a complete description. This is also reflected by the behavior of the cumulative density of states. For the system discussed here, when N and $L \rightarrow \infty$ with $N/L = \rho$ constant by using (53) and (2) we have

$$\frac{\ln D_{\text{mf}}}{\ln D} \approx \frac{1 + \ln \rho}{(1 + \rho) \ln(1 + \rho) - \rho \ln \rho} \equiv \mu(\rho). \quad (55)$$

The function $\mu(\rho)$ is smaller than unity for any finite ρ and tends to unity for $\rho \rightarrow \infty$. Therefore, $D_{\text{mf}}/D \approx D^{\mu(\rho)-1}$ vanishes in the thermodynamic limit.

On the base of our numerical results and the considerations made in the previous Section, the correspondence between quantum chaos of an N -body system and dynamical chaos of its mean-field approximations can be naturally assumed to hold for $N \rightarrow \infty$. This fact is exploited in [23] where the authors consider the chaotic behavior of the same system discussed here when the thermodynamic limit is approached.

ACKNOWLEDGMENTS

We are grateful to J. Bellissard and F. Cesi for enlightening remarks and suggestions. Partial support of INFN, Iniziativa Specifica RM6, is acknowledged.

^a castiglione@roma1.infn.it

^b jona@roma1.infn.it

^c presilla@roma1.infn.it

[1] M. C. Gutzwiller, *Chaos in Classical and Quantum Mechanics* (Springer-Verlag, Berlin, 1990).

[2] O. Bohigas, M. J. Giannoni, and C. Schmit, *Phys. Rev. Lett.* **52**, 1 (1984).

[3] O. Bohigas in *Chaos and Quantum Physics*, edited by M. J. Giannoni, A. Voros, and J. Zinn-Justin, Les Houches Summer School *LII* (North-Holland, Amsterdam, 1991).

[4] A. V. Andreev, O. Agam, B. D. Simons, and B. L. Altshuler, *Quantum chaos, irreversible classical dynamics and random matrix theory*, e-print archive cond-mat/9601001.

- [5] D. C. Meredith, S. E. Koonin, and M. R. Zirnbauer, *Phys. Rev. A* **37**, 3499 (1988).
- [6] G. Montambaux, D. Poilblanc, J. Bellissard, and C. Sire, *Phys. Rev. Lett.* **70**, 497 (1993); D. Poilblanc, T. Ziman, J. Bellissard, F. Mila, and G. Montambaux, *Europhys. Lett.* **22**, 537 (1993).
- [7] R. Berkovits, *Europhys. Lett.* **22**, 493 (1993).
- [8] J.-P. Blaizot and G. Ripka, *Quantum Theory of Finite Systems* (MIT press, Cambridge, 1986).
- [9] G. Jona-Lasinio, C. Presilla, and F. Capasso, *Phys. Rev. Lett.* **68**, 2269 (1992).
- [10] J. C. Eilbeck, P. S. Lomdahl, and A. C. Scott, *Physica* **16D**, 318 (1985); E. Wright, J. C. Eilbeck, M. H. Hays, P. D. Miller, and A. C. Scott, *Physica D* **69**, 18 (1993).
- [11] C. Presilla, G. Jona-Lasinio, and F. Capasso, *Phys. Rev. B* **43**, 5200 (1991).
- [12] W. H. Press, S. A. Teukolsky, W. T. Vetterling, and B. P. Flannery, *Numerical Recipes, the art of scientific computing* (Cambridge University Press, Cambridge, 1992).
- [13] M. Robnik and M. V. Berry, *J. Phys. A* **19**, 669 (1986).
- [14] F. Haake, *Quantum Signatures of Chaos* (Springer-Verlag, Berlin, 1992).
- [15] E. H. Lieb and W. Liniger, *Phys. Rev.* **130**, 1605 (1963).
- [16] P. Castiglione, Laurea Thesis, Universita di Roma “La Sapienza,” unpublished.
- [17] The matrix h is tridiagonal only in the case of Dirichlet boundary conditions whereas in the case of periodic boundary conditions also the corner elements h_{1L} and h_{L1} are nonzero. However, in this last case the lower and upper triangular (LU) decomposition of the matrix h and the subsequent solution of system (26) via the forward- and back-substitution [12] take only $\mathcal{O}(L)$ operations as in the tridiagonal case.
- [18] G. Benettin and L. Galgani, in *Intrinsic Stochasticity in Plasmas*, edited by G. Laval and D. Gresillon (Edition de Physique, Orsay, 1979).
- [19] G. Benettin, M. Casartelli, L. Galgani, A. Giorgilli, and J.-M. Strelcyn, *Nuovo Cimento* **44 B**, 183 (1978).
- [20] F. Calogero and A. Degasperis, *Spectral Transform and Solitons* (North-Holland, Amsterdam, 1982).
- [21] G. P. Berman, E. N. Bulgakov, and G. M. Zaslavsky, *Chaos* **2**, 257 (1992).
- [22] L. G. Yaffe, *Rev. Mod. Phys.* **54**, 407 (1982).
- [23] G. Jona-Lasinio and C. Presilla, *Chaotic properties of quantum many-body systems in the thermodynamic limit*, e-print archive cond-mat/9601056.

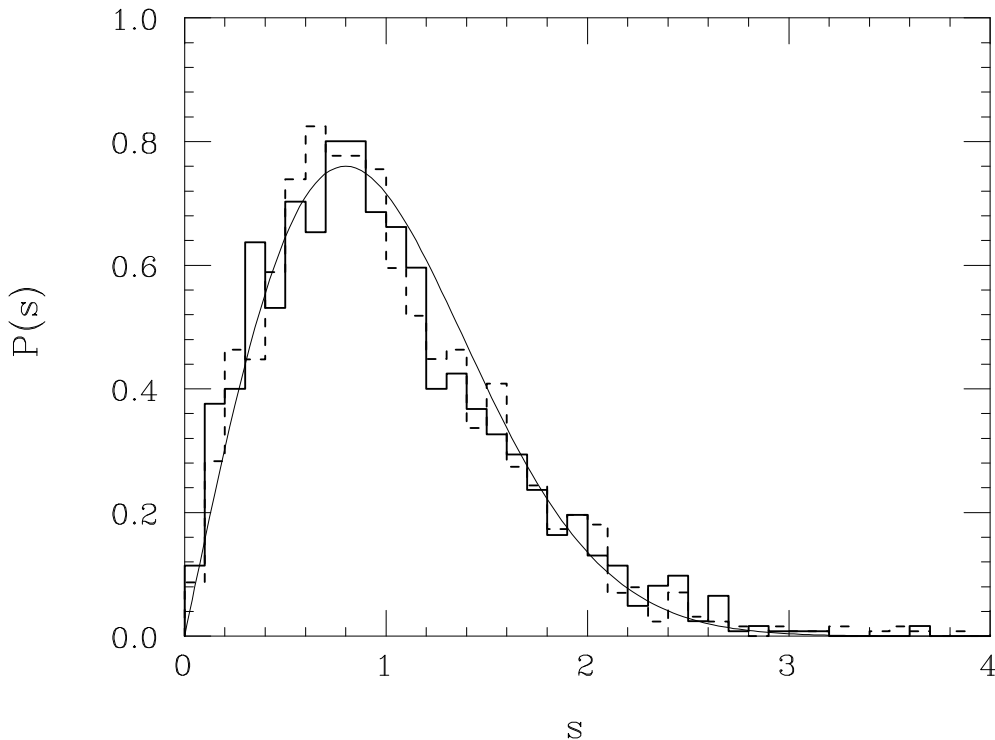


FIG. 1. NNLS distribution $P(s)$ for the system (1) in the uniform case $N = 5$, $L = 9$, $\alpha_j = 0$, $\beta_j = \eta$, and $\gamma_j = \eta$ with $\phi/\phi_0 = 0.3$ and periodic boundary conditions (solid histogram) and $\phi/\phi_0 = 0$ and Dirichlet boundary conditions (dashed histogram). The solid line is the Wigner surmise for the GOE distribution.

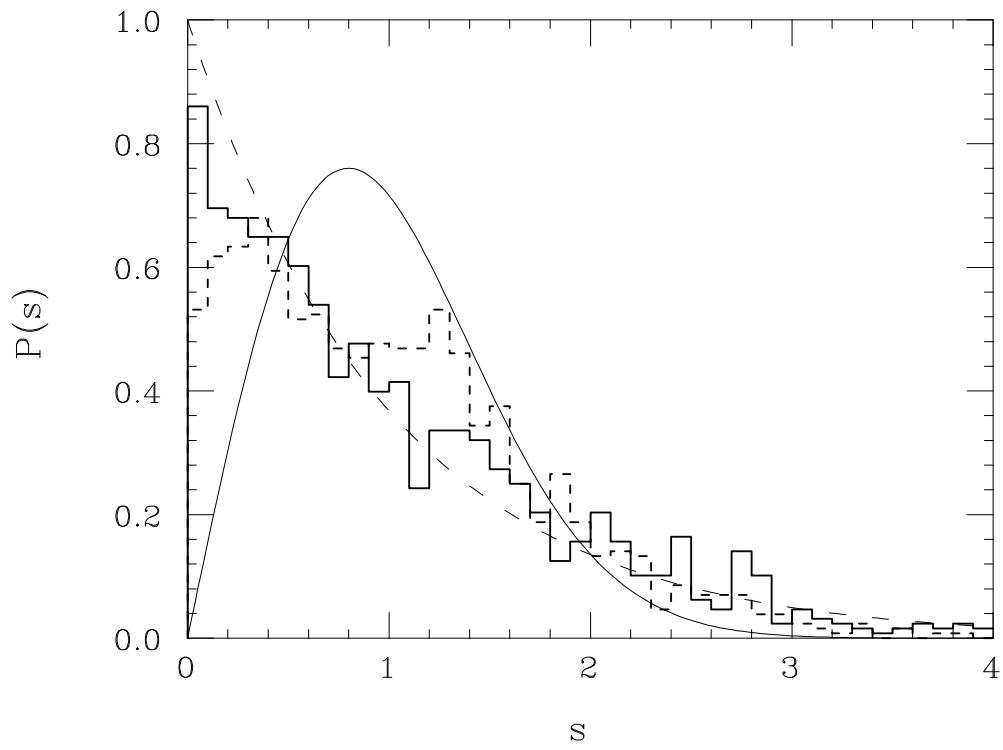


FIG. 2. As in Fig. 1 but without separating the eigenvalues into the appropriate symmetry classes. The dashed line is the Poisson distribution.

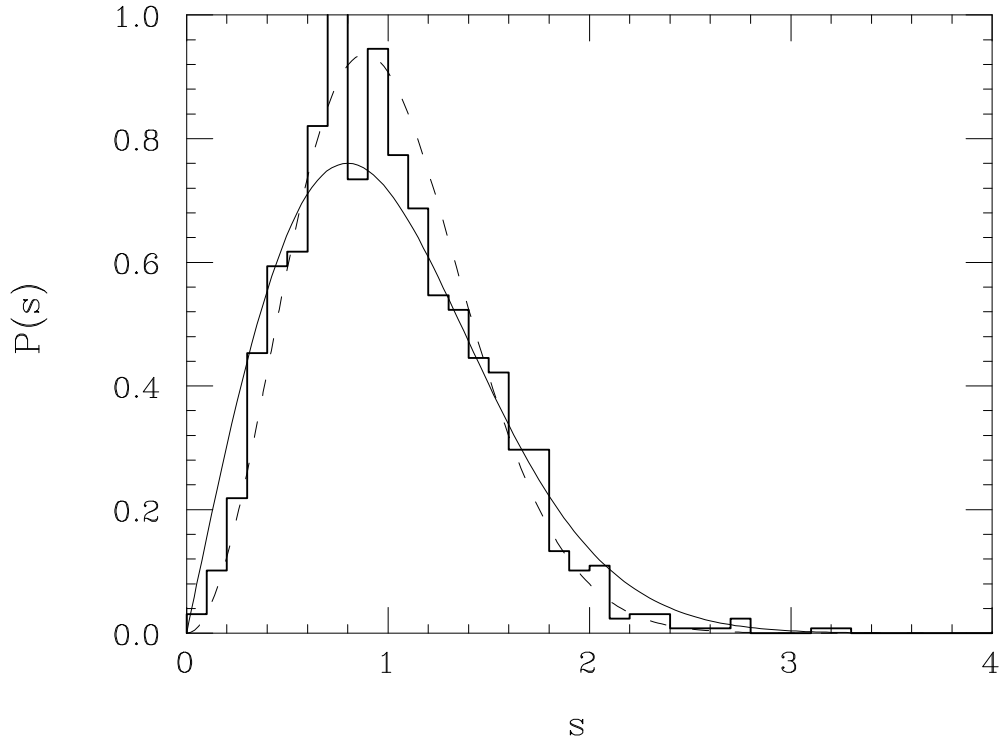


FIG. 3. As in Fig. 1 with periodic boundary conditions but choosing $\alpha_j = 2(N-1)\eta \xi_j$, where ξ_j are arbitrary positive numbers with $\sum_{j=1}^L \xi_j = 1$. The solid and dashed lines are the Wigner surmise for the GOE and GUE distributions, respectively.

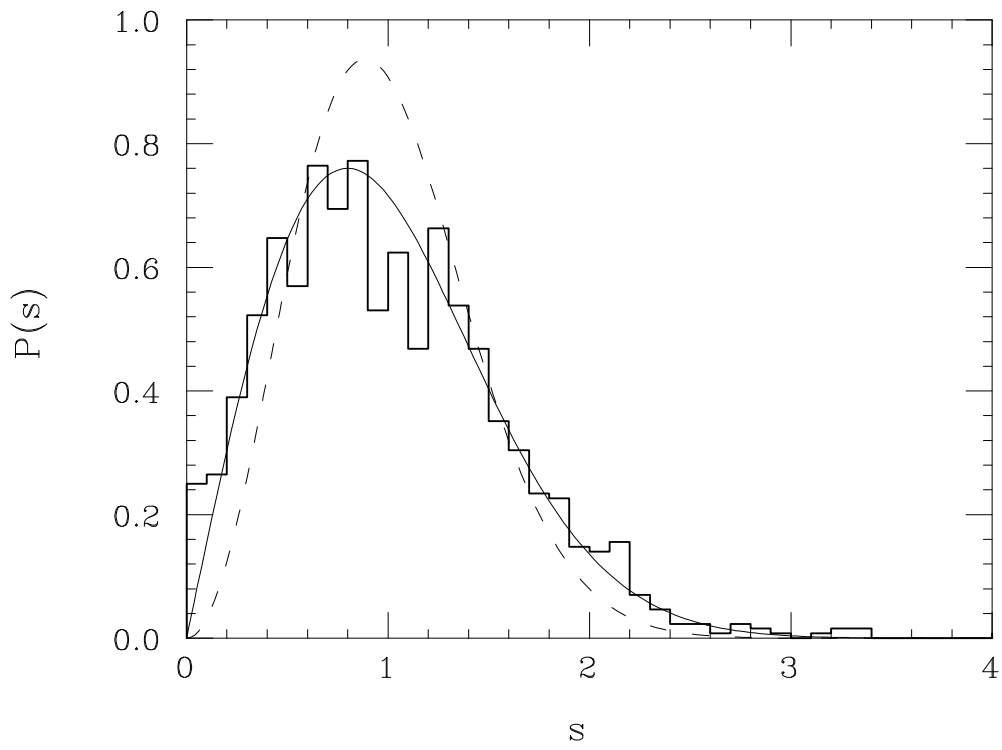


FIG. 4. As in Fig. 3 but choosing $\xi_{j_0-j} = \xi_{j_0+j}$ with j_0 arbitrary.

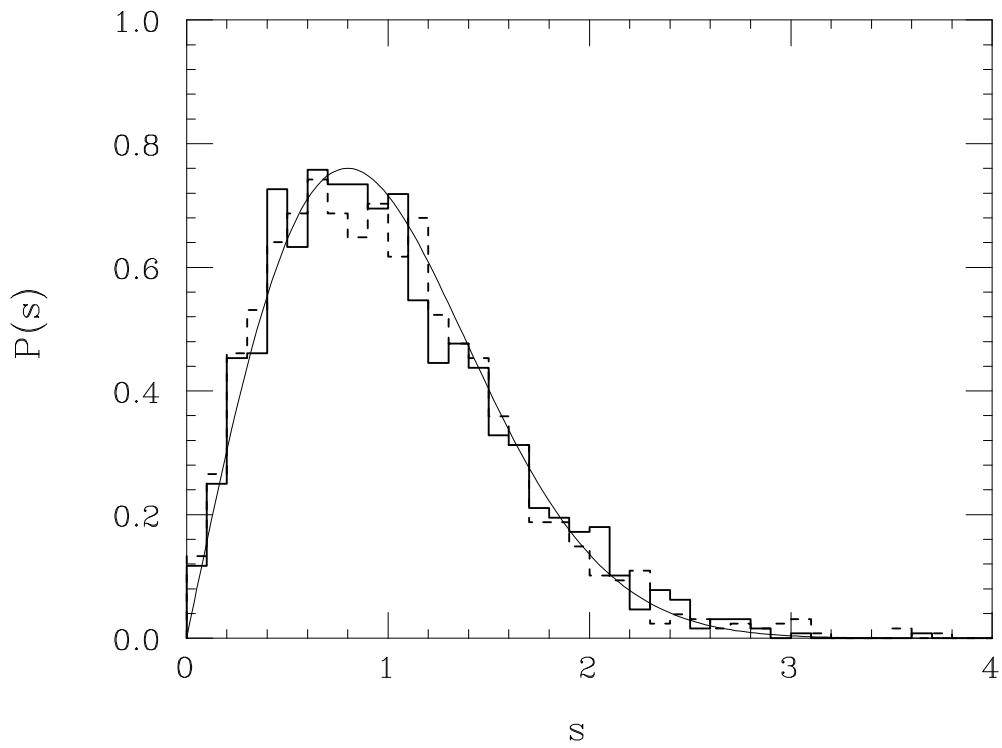


FIG. 5. As in Fig. 1 but choosing $\beta_2 = \beta_3 = 0.5\eta$ and $\beta_j = \eta$ for $j \neq 2, 3$.

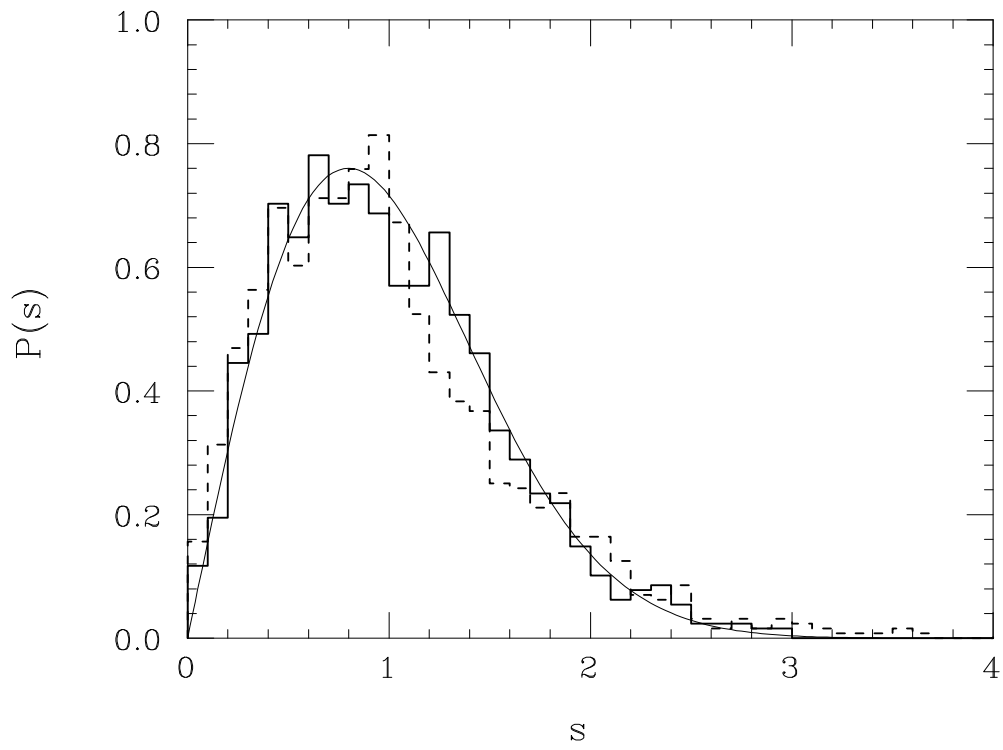


FIG. 6. As in Fig. 1 but choosing $\gamma_j = \eta\delta_{j3}$.

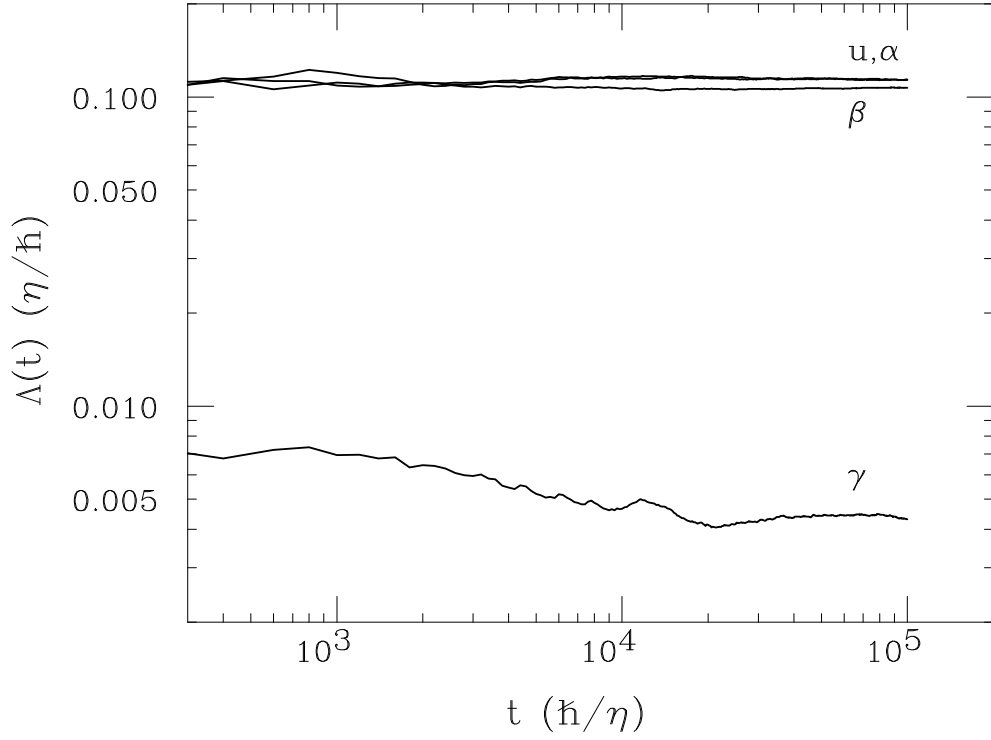


FIG. 7. Maximum Lyapunov exponent for the mean field system (19) with periodic boundary conditions. The curves denoted with u , α , β , and γ , are obtained with the parameters given in Figs. 1, 3, 5, and 6, respectively. The initial conditions $z_j(0)$ and $\delta z_j(0)$ are a set of arbitrary complex numbers satisfying $\|z(0)\|^2 = 1$ and $\text{Re}\langle z(0)|\delta z(0)\rangle = 0$.

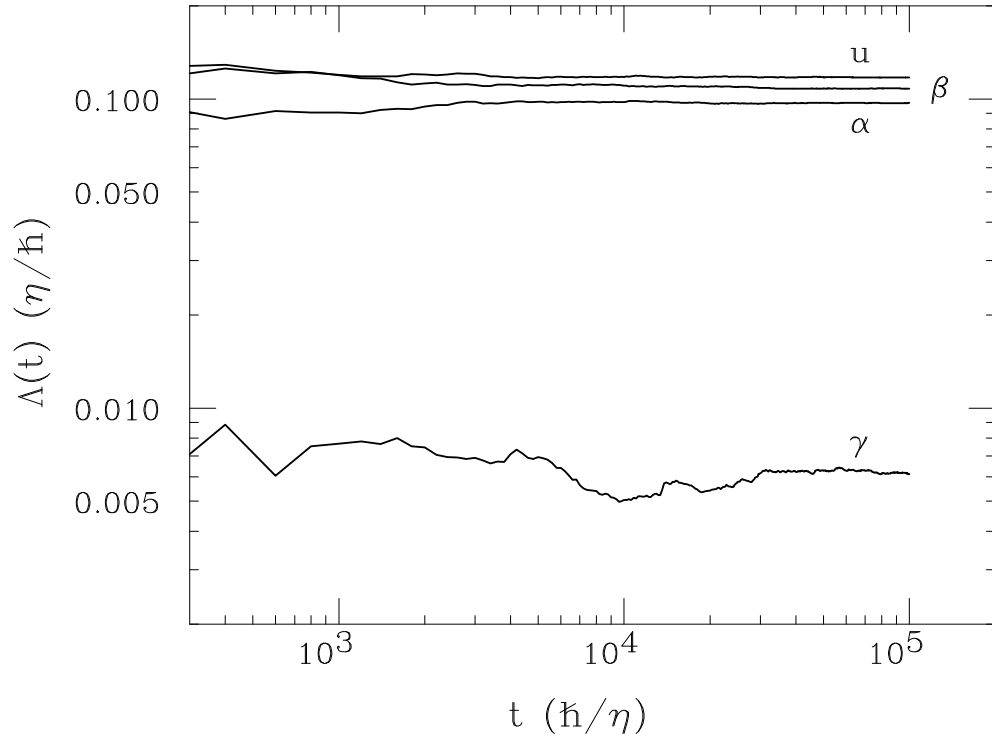


FIG. 8. As in Fig. 7 with Dirichlet boundary conditions.

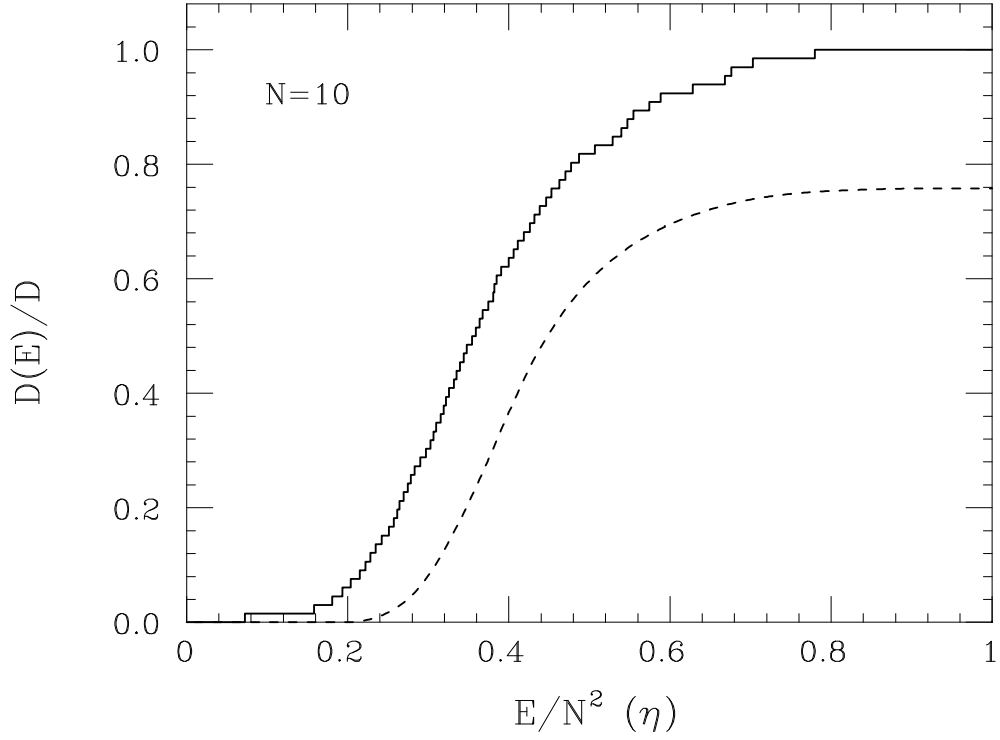


FIG. 9. Cumulative density of states in the case $N = 10$, $L = 3$, α_j , β_j , and γ_j chosen between 0 and η with a random number generator, and with $\phi/\phi_0 = 0$ and Dirichlet boundary conditions. The histogram is the exact result (50) and the dashed line is the mean field approximation (51).

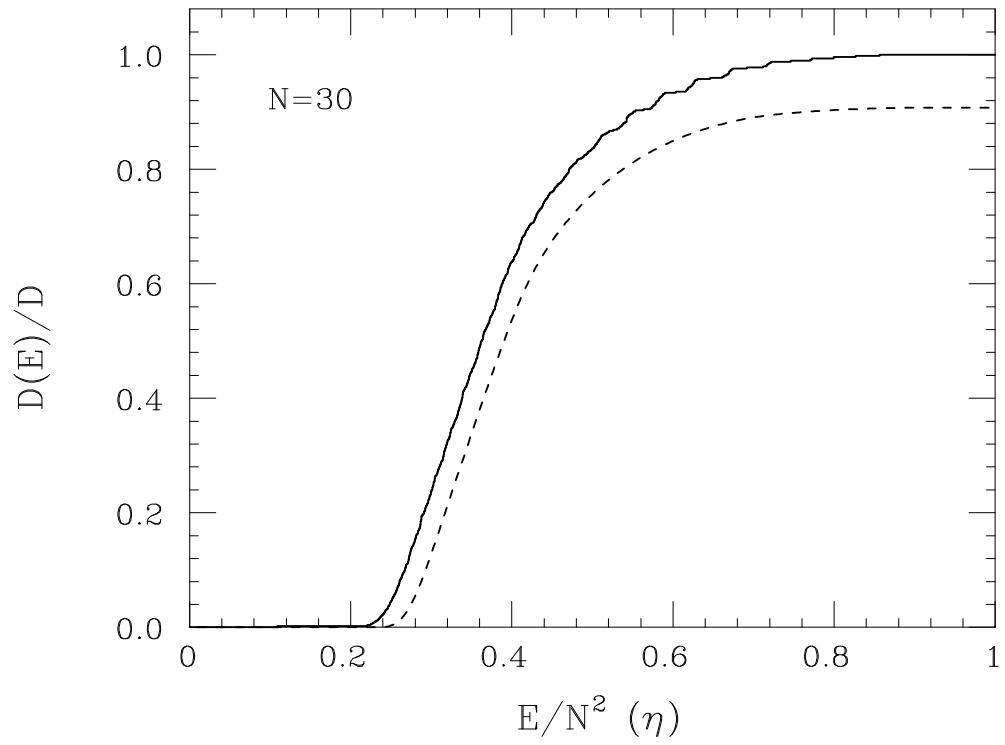


FIG. 10. As in Fig. 9 with $N = 30$.

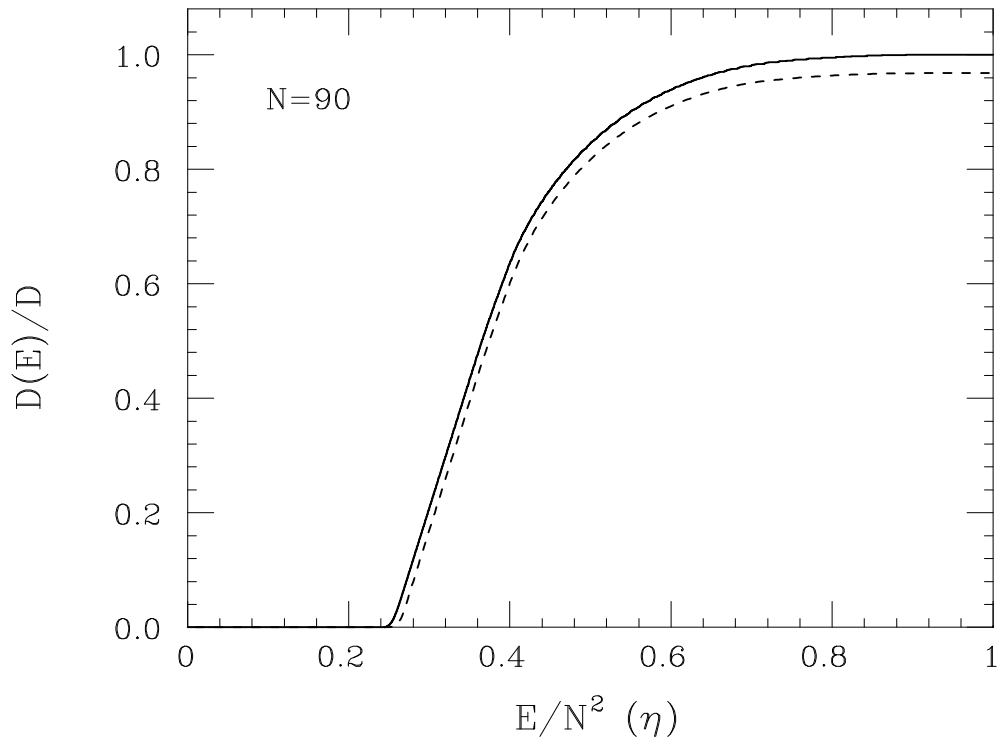


FIG. 11. As in Fig. 9 with $N = 90$.